Effect of stamp design on residual layer thickness and contact pressure in UV nanoimprint lithography

Minqi Yin[1], *Hongwen Sun*[1,2] ✉, *Haibin Wang*[1,2]

[1]*College of Internet of Things Engineering, Hohai University, Changzhou 213022, People's Republic of China*
[2]*Jiangsu Key Laboratory of Power Transmission and Distribution Equipment Technology, Changzhou 213022, People's Republic of China*
✉ *E-mail: hwsun@hhu.edu.cn*

Published in Micro & Nano Letters; Received on 11th July 2017; Revised on 8th February 2018; Accepted on 12th March 2018

Pattern density is an important factor in UV nanoimprint stamp design. Various pattern densities may affect the thickness of the residual layer and its uniformity. This work investigated the effect of pattern density as well as other stamp parameters, including stamp material, stamp thickness and cavity height, on residual layer thickness (RLT), contact pressure, and imprint quality. Two kinds of stamps were designed for simulation, one with detached uniform lines and the other with adjacent non-uniform lines. Results show that areas near the edges of the imprint field in all stamps are the first to achieve high contact pressure. The study observed that long imprint time enables a reduction of RLT after a stable period, particularly obvious with high density. For a long-term imprint of patterns with various densities, flowing behaviour of the residual resist was revealed. These conclusions are beneficial for making guidelines for stamp design in UV nanoimprint lithography.

1. Introduction: UV nanoimprint lithography (UV-NIL) is developing and gaining more attention due to its prospect for industrial production. Several variant processes have been proposed, such as Soft UV-NIL [1], UV enhanced substrate conformal nanoimprint [2], and roll-to-roll liquid transfer imprint lithography [3]. These processes pursue the same optimum performance, namely thin and uniform residual layer, high throughput and high fidelity [4]. Stamp design is an important issue in all these processes. Even though a stamp with evenly distributed pattern density ensures uniform residual layer thickness (RLT) [5], various pattern densities are inevitable when it is applied to manufacturing. It is essential to clarify and quantify the influence of pattern density in UV-NIL.

Most previous reports focused on the effect of imprint process parameters and patterned features on the residual layer in thermal nanoimprint (T-NIL). Rowland *et al.* [6] modelled viscous polymer flowing when imprinting stamps with irregular patterns. They found that both cavity size and pattern width can determine polymer deformation. Moreover, long imprint time and high temperature are helpful to achieve high replication fidelity and uniform residual layer thickness. Bogdanski *et al.* [7] evaluated the influence of pattern size and density in T-NIL. The results proved that residual height relied on pattern size and uniformity of various pattern. Hocheng and Nien [8] reported that the aspect ratio of cavity and pattern density had great influence on the cavity filling, whereas contact friction coefficient had nearly no impact.

The resist of UV-NIL possesses much lower viscosity than that of T-NIL, therefore the inclusion of capillary force makes it complicated to analyse patterning behaviour. As a consequence, a number of simulation methods have been applied in research, including molecular dynamics simulation [9] and finite element simulation [10]. Recent efforts have been made to investigate the effect of pattern density and process parameters in UV-NIL. Lee [11] investigated the impact of imprint pressure on the residual layer thickness in UV-NIL. He found that high imprint pressure, a thin initial layer, and high fluidity of resist help to form a thin and uniform residual layer. In addition, Hiroshima and Atobe [12] observed that smooth flowing of the resist after filling can homogenise the residual layer. They also proposed a capacity-equalised mould to reduce the negative effect of pattern density on imprint quality [13]. By adjusting cavities' height, each area of the mould was made to carry nearly the same capacity for resist filling, so as to create a uniform residual layer despite pattern density variation. However, the complex fabrication process remains a challenge. In a few studies, the imprint contact pressure was taken into consideration [4, 11], but the studies were limited by the lack of real-time measurement of imprint results. In this Letter, a fast simulation technique provided by *Simprint Nanotechnologies Ltd* has employed to analyse the UV-NIL process in detail [14]. By performing a series of simulations, we measured cavity filling, contact pressure, the residual layer thickness in real time, and demonstrated the impact of pattern density on RLT and contact pressure in UV nanoimprint.

2. Modelling and simulation: Prior to performing simulations, stamps and process parameters were prepared in the form of a matrix since *Simprint* software is based on Matlab Compiler Runtime (MCR). In order to clarify the effect of pattern density and surface topography on contact pressure, residual thickness and its uniformity, stamps were divided into two types: with uniform and non-uniform parallel line patterns. Patterns were created by 100×100 matrices to define the surface topography. All lines were 800 µm long. Fig. 1 shows the schematic layout of a $1\,\text{mm} \times 1\,\text{mm}$ quartz mould (Young's modulus: 7.1×10^{10} Pa, Poisson's ratio: 0.17) with pattern density 0.5 and the same line and space (i.e. feature pitch) of 100 nm. Two other stamps were designed with pattern densities of 0.15, 0.3, respectively. A generic UV-NIL resist (surface tension: 0.0275 N/m) was chosen for this case. Fig. 2 presents non-uniform adjacent nanostructures of another $1\,\text{mm} \times 1\,\text{mm}$ quartz stamp with a feature pitch of 100 nm over all pattern regions. Five domains with pattern densities of 0.5, 0.4, 0.3, 0.2 and 0.15 were located at different positions from left to right. In this case, a more popular combination of polydimethylsiloxane (PDMS) mould (Young's modulus: 5.0×10^5 Pa, Poisson's ratio: 0.5) and PAK-01 resist (surface tension: 0.0391 N/m) was added for a comparison with hard mould. The default values of thickness and cavity height of all stamps were set to 500 µm and 200 nm, respectively.

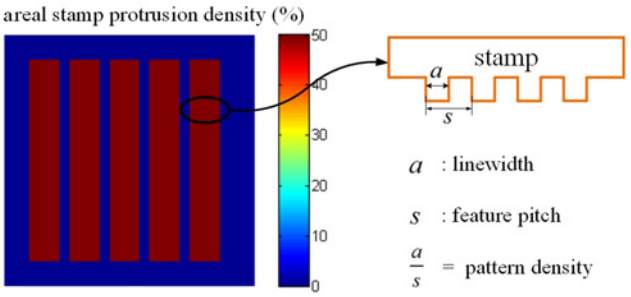

Fig. 1 *Plan view and front view of uniform pattern layout and definition of terminologies*

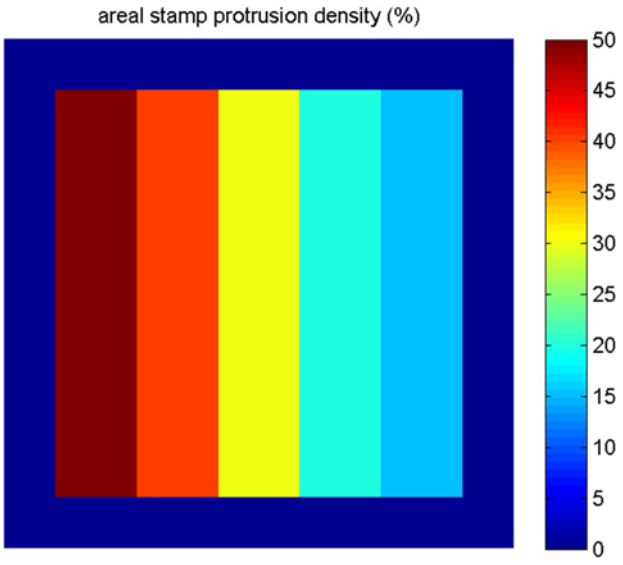

Fig. 2 *Plan view of adjacent non-uniform patterns with various pattern densities of 0.5, 0.4, 0.3, 0.2 and 0.15*

The *Simprint* software is an extension of contact mechanics-based approaches, requiring the detailed design of the process. A function accounting for mechanical deformation at a particular position of resist layer has been offered as follows [15]:

$$p_{g,0}(t) = (1-\nu^2)\int_0^t \frac{1}{D^2}\int_0^D\int_0^D p(x,y,t')\,\mathrm{d}x\,\mathrm{d}y\frac{\mathrm{d}J(t-t')}{\mathrm{d}t'} = (1-\nu^2)\int_0^t p_0(t')\frac{\mathrm{d}J(t-t')}{\mathrm{d}t'}\,\mathrm{d}t' \quad (1)$$

In this function, D, ν, t separately represents the diameter of one spatial period of a notional periodic stamp pattern, Poisson's ratio of resist and time. Depending on a linear viscoelastic model, the above function presents the point-load response of resist with its compliance $J(t)$, imprint pressure $p_0(x, y)$, a dimensionless elastic modulus $(1-\nu^2)$ and average pressure $p_{g,0}(t)$. To be more specific, the assumption of imprint resist as a Newtonian fluid means resist viscosity would keep a constant during the whole calculation. The Newtonian compliance is $J(t) = t/\eta$, where η stands for the viscosity. Besides, imprint pressure for UV-NIL is presented below, which consists of external and capillary pressure [14]:

$$p_0(x,y) = p_{\text{external}}(x,y) + p_{\text{capillary}}(x,y) \quad (2)$$

A silicon substrate (Young's modulus: 1.6×10^{11} Pa, Poisson's ratio: 0.27) and resists, which have been regarded as Newtonian with a constant viscosity of 50 mPa·s, were used in the UV-NIL spun mode. The initial thickness of the resist was 200 nm. The entire UV-NIL process was set to complete within 0.084 s under a uniform pressure of 0.3 MPa. In addition, the contact angle between the stamp and the resist should be specified. Here we assumed that the contact angle was 55°. The completion of simulations offered results of residual layer thickness distribution, cavities' filling proportion and contact pressure.

3. Results and discussion

3.1. Results of the uniform pattern (quartz mould): Owing to the similarity between contact pressure profiles for three pattern densities, the pattern density of 0.3 was selected as an example to illustrate contact pressure evolution. Figs. 3*a* and *c* show the contact pressure distribution for different imprint durations. For the stamp of a certain imprint time, a symmetrical contact pressure distribution was observed. It was found that contact pressure of line structures decreases from pattern edges to the central region. This phenomenon caused by different locations of patterns was obvious at the beginning of the UV-NIL process, as indicated in Fig. 3*a*.

To focus on the vertical analysis of contact pressure, pressure data of the rightmost line pattern was collected. Figs. 3*b* and *d* are two relevant cross-sectional plots corresponding to Figs. 3*a* and *c*, respectively. Note that the dual peak of contact pressure distribution can be easily found in Fig. 3. When UV-NIL was carried out for 0.0118 s, the maximum contact pressure between dual peak was measured as 1.067 MPa and the minimum was 0.9096 MPa. The longitudinal positions of these two points were 285 µm apart. In the other case, the maximum and the minimum contact pressure gradually changed between 0.9507 and 0.9239 MPa, respectively. The distance between these two points was reduced to 215 µm. Longer imprint times lead to reduced inhomogeneity in the contact pressure. Meanwhile, long imprint duration narrows the region of high contact pressure. On the whole, a relatively uniform contact pressure distribution appears with the continuance of UV-NIL, where average contact pressure keeps smoothly

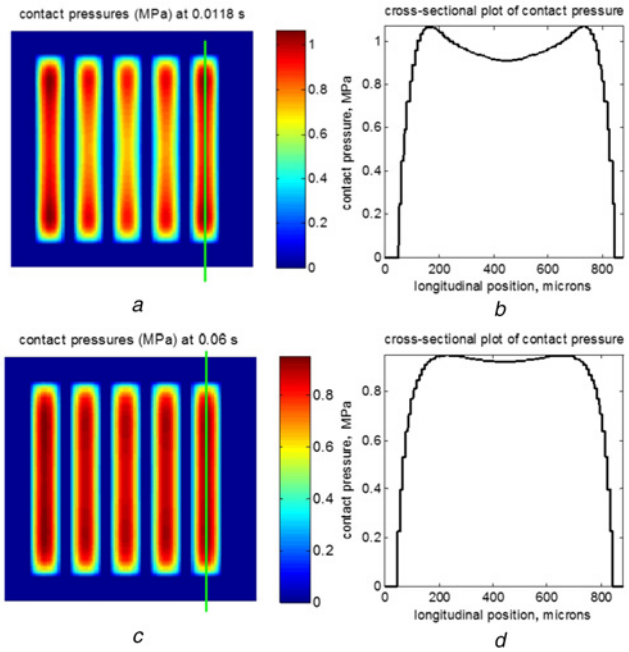

Fig. 3 *Contact pressure distribution with different imprint time*
a At 0.0118 s
b Cross-sectional plot corresponding to the green line segment in (a)
c At 0.06 s
d Cross-sectional plot corresponding to (c)

doi: 10.1049/mnl.2017.0502

decreasing. The concentration of contact pressure in the central region can be considered as an intrinsic property of UV-NIL, which is suspected to be determined by the low viscosity of UV-NIL resist rather than patterns of stamps. This hypothesis would be verified by a study on non-uniform patterns.

Fig. 4 shows a comparison of the RLT evolution for three of the above stamps with various pattern densities. We observed that the higher the pattern density is, the thicker residual layer obtained under the same conditions. The main cause of this phenomenon is that cavity volume is enlarged by decreasing pattern density based on the same feature pitch. Besides, a gradual decrease of RLT cannot be ignored after it has been steady for a long time. This reduction of RLT becomes negligible when pattern density goes smaller. A thinner residual layer can be obtained by a long imprint duration when pattern density is 0.3. The different drops of RLT after 10^{-2} s can be explained by the squeeze of resist, namely the movement to the blue area in Fig. 1. The constant imprint pressure would push more resist out of the patterned area quickly with a thicker residual layer. Actually, the drop would have been sharper if our simulation took the shear thinning effect into consideration. The simulation assumes resist viscosity to be constant during the whole process. However, in fact, the viscosity value deviates from bulk value and changes with resist thickness due to this non-Newtonian effect. Some cases of patterning process, including electro-hydro-dynamic patterning in the work by Amarandei *et al.* [16] and nanoimprinting by Peng *et al.* [17], have proved that there is a threshold of patterns' aspect ratio, and the shear thinning effect would accelerate the growth of structures owing to changes of residual layer viscosity when it goes above threshold. Consequently, the increase in pattern density, which gives rise to higher aspect ratio, would make drops more obvious after 10^{-2} s in reality.

3.2. Results of the non-uniform pattern (quartz mould): Fig. 5*a* shows a false colour map of the cavity filling for a stamp with five different pattern densities. We found that a high pattern density brings a high filling ratio when holding feature pitch constant. According to previous research [18], wider cavities (i.e. low pattern density) produce a larger volume of the cavity to be supplied, but they enable resist to fill faster in general. Combined with the above conclusion, this result indicates that a high cavity

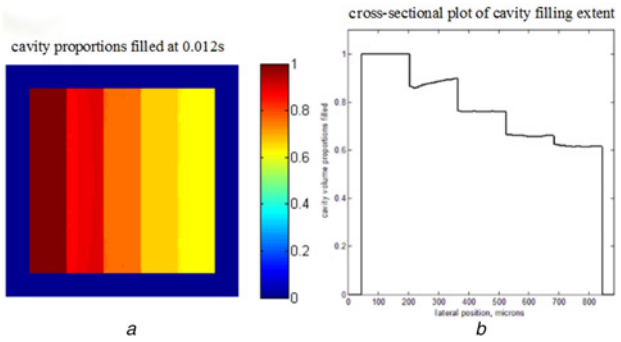

Fig. 5 *Cavity filling extent of neighboring non-uniform patterns*
a Profiles of cavity filling proportions at 0.012 s
b Horizontal cross-sectional plot of cavity filling extent

filling proportion is mostly decided by small cavity volume despite its low filling speed. A curve depicting cavity filling proportions is shown in Fig. 5*b*, which indicates that there is a rising trend of cavity filling extent in the region with a pattern density of 0.4 from its left boundary to the right boundary. Some slight fluctuations appear in regions with a pattern density of 0.2 and 0.15, especially near their boundaries. Both phenomena prove that proximity effect also occurs in UV-NIL, which denotes that the distribution of resist in cavities becomes asymmetrical when protrusions of different densities are separated by a close distance.

The evolution of contact pressure distribution is illustrated in Fig. 6. At the outset, the region with pattern density 0.5 accounts for the highest proportion of contact pressure, whose peak is 1.27 MPa. The central region with 0.4 pattern density has far less pressure. The contact pressure in the regions with a pattern density of 0.3, 0.2, and 0.15 ranges from 0.445 to 0.547 MPa, and shows the 'dual peak' behaviour. For an imprint time of 0.0247 s, longitudinal dual peaks of contact pressure still remain, as shown in Fig. 6*b*. The left peak is about 0.739 MPa and the right one is 0.68 MPa. Despite low contact pressure of 0.42 MPa in the central region of the stamp, a relatively uniform distribution is obtained.

For a long period of UV nanoimprint, we observed apparent homogenisation of contact pressure between the stamp and resist.

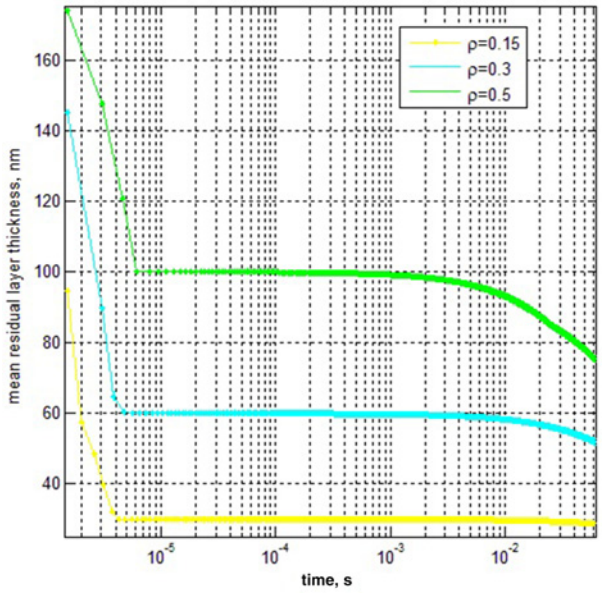

Fig. 4 *Evolution of average residual layer thickness with three pattern densities of 0.15, 0.3, 0.5*

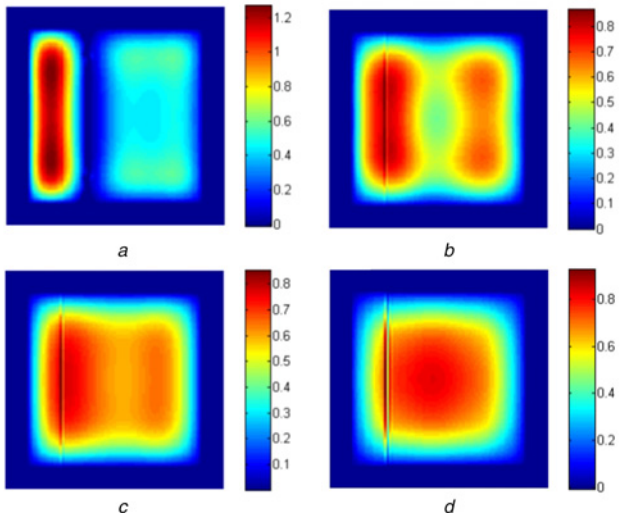

Fig. 6 *Profiles of contact pressure of non-uniform patterns (MPa)*
a At 0.00825 s
b At 0.0247 s
c At 0.0333 s
d At 0.0667 s

As illustrated in Figs. 6*c* and *d*, from 0.0333 to 0.0667 s of the simulated process, the distribution becomes more uniform and at last, most of the pressure gathers at the centre of the imprint field. Moreover, the dual peak of contact pressure is converted into a single peak, which has a value of 0.828 MPa in Fig. 6*d*. There is a noticeable pressure gap at the boundary between regions with a pattern density of 0.4 and 0.5. As the process is progressing, the gap grows larger, and the maximum difference was measured as 0.26 MPa in Fig. 6*d*. At the position symmetrical to the gap, contact pressure changes smoothly near the boundary between regions with a pattern density of 0.2 and 0.15. In contrast, this indicates that high uniformity of pressure benefits from less variance in adjacent pattern densities. Through the whole process, the average contact pressure keeps decreasing and uniformity of pressure tends to be improved. Generally, protrusions with high density account for most of the contact pressure, and the rest is distributed to areas near the edges of imprint field. Finally, prolonging the process changes the dual peak of contact pressure into a single peak in the vertical direction. It also enables pressure to gather at the centre of stamp regardless of various pattern densities.

Residual layer thickness profiles for five different imprint times are shown in Fig. 7. Some singular points near lateral position 200 µm verify that the contact pressure gap between domains causes exceptions in RLT. For the imprint duration of 0.12 s, the thickest part of the residual layer is at pattern density of 0.2–0.3. The peak of RLT keeps moving to larger values of pattern density until 0.06 s in the simulation, located at pattern density around 0.4–0.5. At 0.084 s, the transfer of RLT peak to the central region of field occurs, which finally results in a stable and symmetrical residual layer. Obviously, this phenomenon of resist flowing is induced by variation of pattern density, where residual resist flows from the region with a low pattern density to that with a high pattern density, and reflows to the centre of the patterned field at the end of the long-term process. However, the residual layer near left and right edges of the patterned field (i.e. lateral position of 40 and 840 µm, respectively) are exceptions in Fig. 7, which is always thinner than that of other areas. This edge effect on RLT remains during the whole process. We observed that there is a sharp decrease in thickness at the right edge of the field, which is measured as 4 nm and can be viewed as another singular point in the residual layer. Outside and near the edges of imprint field, an increase of residual layer thickness was observed, where the RLT is 289 and 265 nm, respectively, at the left and right sides. These values are much larger than the initial resist thickness of 200 nm, which means a small amount of resist was expelled from patterned regions and then gathered at the outer edges of the stamp.

Hiroshima and Atobe [12] found that resist flows only at the region boundary from regions with low density to that with high density in UV nanoimprint by a stamp with both different pattern densities and feature pitches, which can be complemented by our simulation results. The residual resist would flow across the whole patterned field from the region of low pattern density to that of high density if keeping feature pitch constant.

3.3. Results of the non-uniform pattern (PDMS mould)

RLT distribution of a PDMS stamp is obviously different from that of a quartz stamp. Comparing with Figs. 8*a* and *b*, it is illustrated that process using a PDMS mould leads to unevenly distributed RLT. The RLT differences range from approximately 12 to 26 nm. In contrast, a process using quartz mould leaves a relatively more uniform RLT.

The influence of stamp thickness is demonstrated in Fig. 9, where the thickness smoothly increases from 200 µm to 1 mm. The mean RLT remains constant at about 76 nm; the standard deviation of RLT remains the same despite the increasing stamp thickness. On the other hand, the cavity filling ratio gradually grows to its peak of 53.7% when the stamp thickness reaches 800 µm. This means a growth of stamp thickness has a slight positive effect on cavity filling process, while RLT maintains nearly unchanged.

Cavity height is another significant factor in achieving a high imprint quality. With cavity heights changing from 80 to 180 nm, mean RLTs and their standard deviations are shown in Fig. 10. With the increase of the cavity height, mean RLT declines from 138 to 88 nm smoothly and nearly follows a linear trend. This means higher cavities of different pattern densities would contribute to a more non-uniform residual layer, though reducing the mean value of RLT.

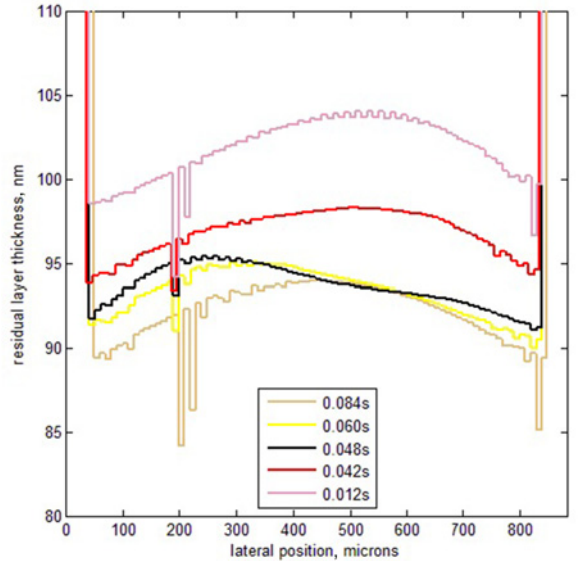

Fig. 7 *Evolution of residual layer thickness with different imprint time*

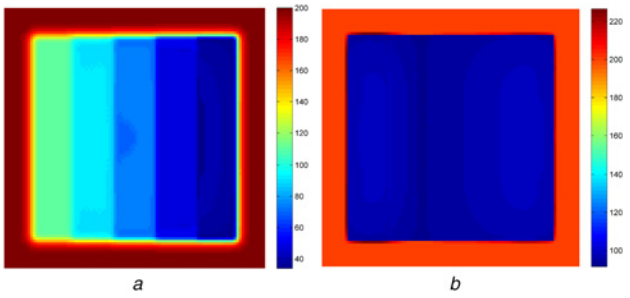

Fig. 8 *RLT distribution of*
a PDMS stamp
b Quartz stamp

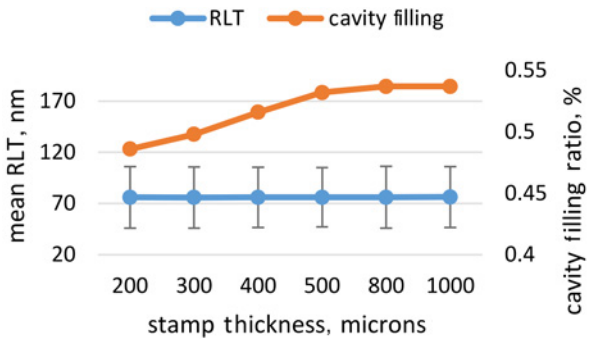

Fig. 9 *Evolution of mean RLT and cavity filling proportion with various stamp thickness*

doi: 10.1049/mnl.2017.0502

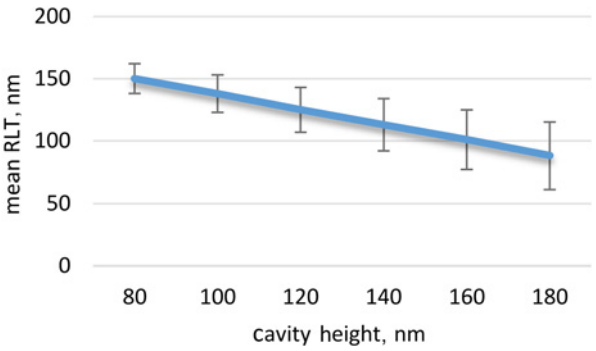

Fig. 10 *Evolution of mean RLT with different cavity heights*

4. Conclusion: The influence of pattern density variation and imprint duration in UV nanoimprint was investigated by means of fast simulations. There is a dual peak of contact pressure in the vertical direction with a stamp of line structures pressed for a short time. Long imprint duration relieves this dual peak phenomenon and homogenises the contact pressure. This implies that pattern edges are the first area to make contact with resist. Residual layer thickness is enabled to have a reduction after being stable by extension of imprint duration, which can be exaggerated via a higher pattern density with feature pitch a constant. For a certain imprint time, a higher pattern density result in a higher filling ratio, but the proximity of patterns with different densities would affect cavity filling extent. In imprinting non-uniform patterns, we found that the edges of the field with higher densities occupied a large proportion of contact pressure at the beginning, and later pressure of other regions near pattern edges grows smoothly. All of them produce 'dual peak' within contact pressure. The pressure gap at the region boundary indicates that uniform pattern density facilitates a uniform pressure distribution. From RLT evolution of uniform patterns, the flowing behaviour of residual resists can be illustrated. At regions of same feature pitch but with various pattern densities, residual resist flows from regions with low density to that with high density, and gathers at the central area at the end of the process. At the inner edge of patterned field, RLT reaches a low point but achieves a maximum at the outer edge since a small quantity of resist is expelled through pattern edges. A PDMS stamp induces a more non-uniform residual layer than a conventional hard stamp. Increasing stamp thickness has a minor positive effect on resist filling. The uniformity is influenced by the cavity height, where a thicker but more uniform residual layer is caused by decreasing the cavity height. Based on these conclusions, imprint quality can be improved by controlling parameters like feature pitch, pattern density and imprint time.

5. Acknowledgments: This research was supported by the Changzhou Sci&Tech Program (grant no. CJ20179036) and the Fundamental Research Funds for the Central Universities. This work also supported by NSFC through Hohai University under grant no. 61504038.

6 References

[1] Glinsner T., Lindner P., Plachetka U., *ET AL.*: 'Soft UV-based nanoimprint lithography for large-area imprinting applications'. Proc. SPIE, Emerging Lithographic Technologies XI, San Jose, USA, February 2007, vol. 6517, p. 651718

[2] Ji R., Hornung M., Verschuuren M.A., *ET AL.*: 'UV enhanced substrate conformal imprint lithography (UV-SCIL) technique for photonic crystals patterning in LED manufacturing', *Microelectron. Eng.*, 2010, **87**, (5), pp. 963–967

[3] Moro M., Taniguchi J.: 'Removal of residual layer by liquid transfer imprint lithography using roll-to-roll UV-NIL', *Microelectron. Eng.*, 2015, **141**, (1), pp. 112–116

[4] Scheer H.C., Papenheim M., Dhima K., *ET AL.*: 'Aspects of cavity filling with nano imprint', *Microsyst. Technol.*, 2015, **21**, (8), pp. 1595–1605

[5] Bender M.D., Fuchs A., Plachetka U., *ET AL.*: 'Status and prospects of UV-nanoimprint technology', *Microelectron. Eng.*, 2006, **83**, (4), pp. 827–830

[6] Rowland H.D., King W.P., Sun A.C., *ET AL.*: 'Simulations of non-uniform embossing: The effect of asymmetric neighbor cavities on polymer flow during nanoimprint lithography', *J. Vac. Sci. Technol. B*, 2005, **23**, (6), pp. 2958–2962

[7] Bogdanski N., Wissen M., Moellenbeck S., *ET AL.*: 'Challenges of residual layer minimisation in thermal nanoimprint lithography'. Proc. SPIE, 23rd European Mask & Lithography Conf., Grenoble, France, May 2007, vol. 6533, p. 65330Q

[8] Hocheng H., Nien C.C.: 'Numerical analysis of effects of mold features and contact friction on cavity filling in the nanoimprinting process', *J. Micro/Nanolith. MEMS MOEMS*, 2006, **5**, (1), pp. 139–144

[9] He Y., Sun T., Yuan Y., *ET AL.*: 'Molecular dynamics study of the nanoimprint process on bi-crystal Al thin films with twin boundaries', *Microelectron. Eng.*, 2012, **95**, (1), pp. 116–120

[10] Liu D.S., Tsai C.Y., Lu Y.T., *ET AL.*: 'Finite element method investigation into nanoimprinting of aluminum/polyimide bi-layer substrates', *Microelectron. Eng.*, 2010, **87**, (11), pp. 2361–2367

[11] Lee H.: 'Effect of imprinting pressure on residual layer thickness in ultraviolet nanoimprint lithography', *J. Vac. Sci. Technol. B*, 2005, **23**, (3), pp. 1102–1106

[12] Hiroshima H., Atobe H.: 'Homogeneity of residual layer thickness in UV nanoimprint lithography', *Jpn. J. Appl. Phys.*, 2009, **48**, (6), pp. 1–4

[13] Hiroshima H.: 'Nanoimprint with thin and uniform residual layer for various pattern densities', *Microelectron. Eng.*, 2009, **47**, (10), pp. 8098–8100

[14] Taylor H.K., Wong E.J.: 'Fast simulation of nanoimprint lithography: modeling capillary pressures during resist deformation'. 10th Int. Conf. Nanoimprint and Nanoprint Technology, Jeju, Korea, 2011, pp. 1–2

[15] Taylor H.K., Boning D.S.: 'Towards nanoimprint lithography-aware layout design checking'. Proc. SPIE, Design for Manufacturability through Design-Process Integration IV, San Jose, USA, April 2010, vol. 7641, p. 76410U

[16] Amarandei G., Dwyer C.O., Arshak A., *ET AL.*: 'Fractal patterning of nanoparticles on polymer films and their SERS capabilities', *ACS Appl. Mater. Inter.*, 2013, **5**, (17), pp. 8655–8662

[17] Peng H.G., Kong Y.P., Yee A.F.: 'Relaxation kinetics of nanostructures on polymer surface: effect of stress, chain mobility, and spatial confinement', *Macromolecules*, 2009, **43**, (1), pp. 409–417

[18] Rowland H.D., Sun A.C., Schunk P.R., *ET AL.*: 'Impact of polymer film thickness and cavity size on polymer flow during embossing: toward process design rules for nanoimprint lithography', *J. Micromech. Microeng.*, 2005, **15**, (12), pp. 2414–2425